https://doi.org/10.48048/tis.2022.4496

Adaptive Phase Lead Compensation for Model Uncertainties Problem of Autonomous Land Vehicles in Irregular Milieus

Rahma Boucetta[*], Radwen Bahri and Saloua Bel Hadj Ali

Department of Physics, Sciences Faculty of Sfax, University of Sfax, Sfax 3000, Tunisia

([*]Corresponding author's e-mail: boucetta.rahma@gmail.com)

Received: 24 July 2020, Revised: 20 November 2021, Accepted: 30 November 2021

Abstract

In this research paper, digital and analog adaptive phase lead control schemes for model uncertainties problem are proposed to Autonomous Land Vehicles (ALV) in highly irregular environments. The developed compensators are used to improve control performances and maintain robustness against uncertainties and external disturbances. To consider real soil changes and irregularities, 2 approaches are addressed: The 1st approach is a digital phase lead controller synthesized to keep closed loop performances in spite of analog system uncertainties. The 2nd control strategy rests on adaptive analog compensator to reduce model uncertainties impact using programmable resistors. Both control approaches are theoretically detailed, and then implemented on a test bed to compare real time results in terms of accuracy and rapidity in the model uncertainties case.

Keywords: Model uncertainties, Adaptive control, Phase lead compensator, Autonomous Land Vehicles

Introduction

ALV stand for vehicles that operate while in continuous contact with the ground and without onboard human attendance. The ALV serve for several applications where it may be inconvenient, dangerous, or impossible to have a human operator attendance [1]. An ALV is essentially an autonomous robot that operates on the basis of artificial intelligence technologies without the need for a human controller. The vehicle invests its sensors to develop some limited understanding of the environment, which is subsequently used by control algorithms to determine the next action to take in the context of a human provided mission goal. This eliminates thoroughly the need for any human to maintain the servile tasks that the ALV is performing [2].

An ALV needs to be capable of gathering information about the environment, to detect objects of interest in order to avoid situations that are harmful to people, etc. In fact, autonomous learning of land robots includes the ability to learn or gain new capacities without external assistance, to adjust strategies based on surroundings, to adapt to these environments without outside assistance and to develop a sense of ethics regarding mission goals [3].

In natural environments, ground is highly non-homogenous, hazardous and permanently changing, which makes ALV subject to multiple phenomena consisting a main reason of performance degradation because of wheel-ground contact change. The continuous contact between wheels and ground can affect directly internal parameters of the ALV system [4]. To settle this awkward problem, 2 control approaches were elaborated in the literature review. The 1st one relies upon robust control, and the 2nd solution rests on the adaptive techniques of control [5].

A discrete time sliding mode approach was set forward by [6] to control mobile robots with uncertainties in the dynamic model. This work was corroborated by experimental results. Dong and Kuhnert [7] presented a robust adaptive control of nonholonomic mobile robot with parameter and nonparameter uncertainties. A backstepping case study was developed by [8] for the tracking control of mobile robots. Park *et al.* [9] introduced an adaptive neural sliding mode control of nonholonomic wheeled mobile robots with model uncertainties. Kim *et al.* [10] designed a robust adaptive dynamic controller applied to nonholonomic mobile robots under model uncertainties and disturbances. Khalaji [11] addressed the trajectory tracking problem of nonholonomic vehicles in the presence of uncertainties.

In this research paper, 2 adaptive phase lead controllers are synthesized in analog-analog and analog-digital concepts so as to compensate the ground change effect on internal parameters of the ALV

systems. This paper is structured as follows. Section 2 identifies the problem of uncertainties of ALV model for different types of soils. The principle of the classical phase lead compensator is displayed in Section 3. The analog-digital adaptive phase lead controller is exhibited in Section 4. In Section 5, the analog-analog form of an adaptive phase lead compensator is tackled with real time tests for different uncertainty cases to compare results and demonstrate control performances. Eventually, the last section wraps up the conclusion and displays pertinent concluding remarks.

Model uncertainties

To examine wheel-ground contact, a test bed is performed in the MACS Laboratory at the University of Gabes with a wheel fixed to a DC motor shaft and mounted on a metal stem. At the end of the latter, we incorporated an electronic system, namely an Arduino card, an IMU inertial sensor and a power board for the motor control, **Figure 1**.

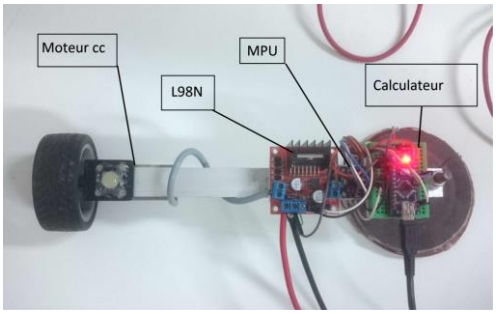

Figure 1 Open-loop test bed.

The types of soils chosen for experiments are wood, sand and laboratory tiling. The same voltage is supplied to the DC motor input to produce a wheel rotation around the fixed measurement system, and extract the corresponding angular velocity response. The different step responses of the angular velocity for the 3 soils are handled with MATLAB and illustrated in **Figure 2**. The identified model deduced from the various outputs do not have the same parameters, which indicates that the system needs to be performed with an adaptive controller.

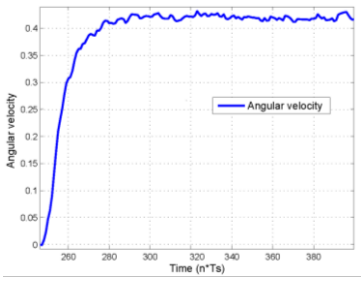

(a) Wheel-wood

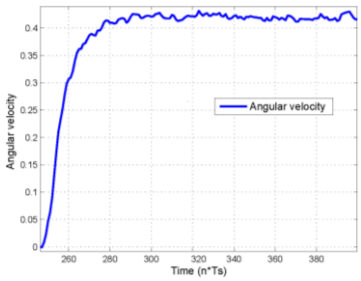

(b) Wheel-sand

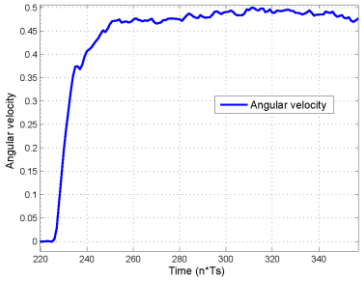

(c) Wheel-tiling

Figure 2 Open-loop responses for different soils.

Phase lead control

The phase lead controller or compensator is an approximate form of the Proportional-Derivative (PD) corrector, that is physically impractical because of the unverified causality hypothesis. Indeed, the phase lead controller allows a phase margin increase at 0 dB by introducing a positive phase owing to derivative impact to improve stability. This form of controller allows likewise a bandwidth enlargement to enhance rapidity in closed-loop [13]. The transfer function of the phase lead controller is expressed as:

$$C(p) = K_c \frac{1+aTp}{1+Tp}, \quad \text{a>1} \tag{1}$$

It can give a maximum phase advance corresponding to:

$$\varphi_{c,\max} = \arcsin \frac{a-1}{a+1}, \quad \varphi_{c,\max} > 0 \tag{2}$$

and an equivalent pulsation as:

$$\omega_{c,\max} = \frac{1}{T\sqrt{a}} \tag{3}$$

To carry out concretely a phase lead controller, an electronic circuit composed of operational amplifiers, resistors and capacitors is incorporated in **Figure 3**.

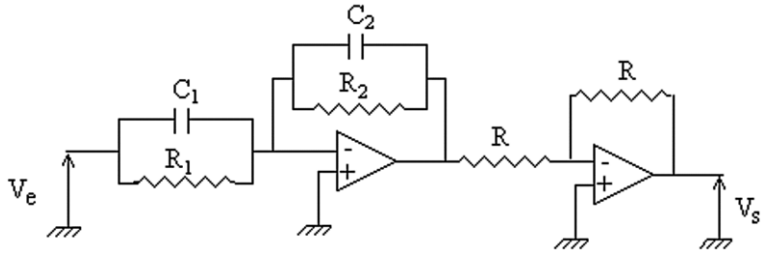

Figure 3 Electronic circuit of a phase lead controller.

The parameters of the controller are determined from resistors and capacitors values in terms of:

$$a = \frac{R_1C_1}{R_2C_2}, \quad K_c = \frac{R_2}{R_1}, \quad T = R_2C_2 \tag{4}$$

Analog-digital adaptive lead control

An adaptive controller is basically synthesized in a time domain either with some criteria minimization for parameters adjustment or a time identification to update system parameters with a desired reference model. However, the lead control synthesis is mostly harmonic using Bode or Black diagrams to improve stability with phase margin increase. To obtain an adaptive version of the phase lead controller that can hold its main properties of stability and is capable of maintaining efficiency during process re-parametrization around a nominal value, a pole placement approach is applied to control the system position. The desired model behaves as a 2nd order system with a damping factor $\xi = 0.707$ and a proper pulsation $\omega_n = 3$ rad/s. The transfer function of the system has the following expression:

$$G(p) = \frac{K}{p(1+\tau p)} \qquad \tau = 0.3s, \; K = 3 \tag{5}$$

The gain K can vary from 1 to 5. The lead controller has the transfer function stated in Eq. (1). The closed-loop of the system position is illustrated in **Figure 4**.

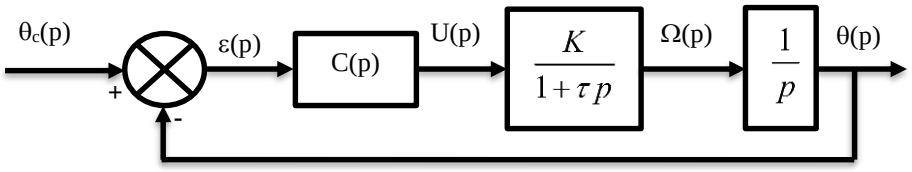

Figure 4 Closed-loop control of the position.

The transfer function of the closed-loop is expressed as:

$$H_{BF}(p) = \frac{\theta(p)}{\theta_c(p)} = \frac{C(p)G(p)}{1+C(p)G(p)} \tag{6}$$

To compensate the dominant pole, an adequate choice needs to be imposed as $\tau = aT$, to obtain:

$$KK_c = \omega_n / 2\xi \text{ and } T = KK_c / \omega_n^2 \tag{7}$$

The values of different parameters of the controller are provided by:

$$T = 0.2357,\ a = 1.2726,\ K_c = 0.7013 \tag{8}$$

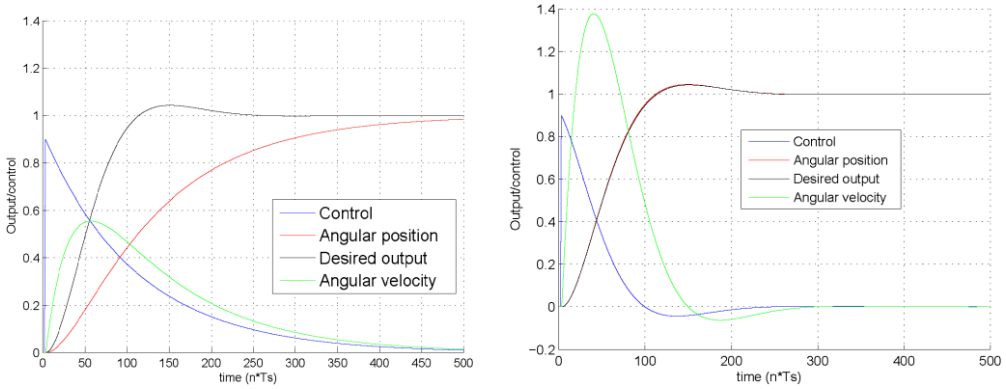

(a) K = 1 (b) K = 3

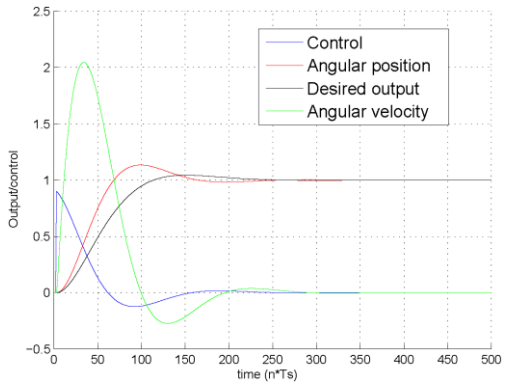

(c) K = 5

Figure 5 Closed-loop responses for various gains.

Figure 5 displays different step responses of angular position and velocity of the closed-loop system concerning K = 1, 3 and 5 cases. If the controller parameters are maintained constant, the slightest variation of the gain K can degrade rapidly the closed-loop performances in stability for a high value of K, and in rapidity for a low value of K as well. Furthermore, the time constant τ can be a subject of variation and induces effects on dynamics, and accordingly on parameters' change in the closed-loop. To resolve these problems, an indirect adaptive approach is used as plotted in **Figure 6**.

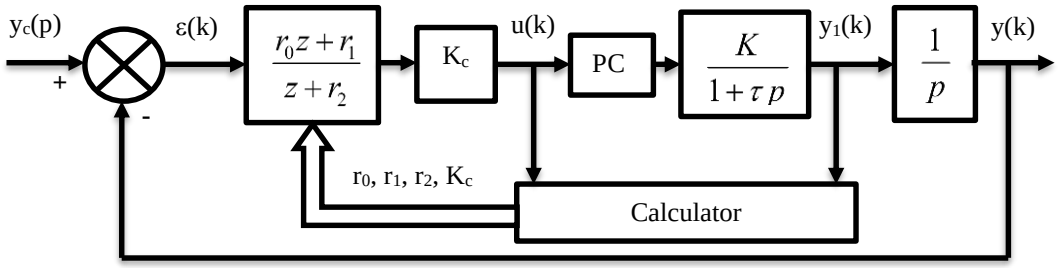

Figure 6 Structure of the proposed controller.

Parametric identification with Model Reference Control (MRC) scheme allows to determine process parameters in each sample period following with an update of parameters [12,13]. In digital configuration, the transfer function of the phase lead controller can be determined as:

$$C(z) = Z(K_c \frac{1+aTp}{1+Tp}) B_0(p) = K_c \frac{r_0 z + r_1}{z + r_2} \quad (9)$$

$B_0(p)$ is a 0-order hold depicting the DAC. To isolate the integration presented in the system transfer function, 2 methods can be adopted: The 1st method consists in transferring integration to the system output as:

$$y(k) = \frac{B(q^{-1})}{A(q^{-1})(1-q^{-1})} u(k) \quad (10)$$

$$y_1(k) = (1-q^{-1}) y(k) = \frac{B(q^{-1})}{A(q^{-1})} u(k) \quad (11)$$

The 1st terms, namely output derivatives, are invested to specify a_i, and b_i parameters.

The 2nd method relies on carrying forward the integration in the input. A new input arises in the 2nd member of Eq. (10) as:

$$y(k) = \frac{B(q^{-1})}{A(q^{-1})} \frac{u(k)}{(1-q^{-1})} = \frac{B(q^{-1})}{A(q^{-1})} u_1(k) \quad (12)$$

The 1st method amplifies the noise and maintains the fullness of the input whereas the 2nd one is quite the opposite. Since the position signal is not noisy, the 1st method is adopted to develop the adaptive phase lead controller in an analog-digital scheme. The passage from the discrete model to the continuous equivalent is based on the 2 following assumptions:

$$K = \frac{b_1}{1+a_1} \text{ and } \tau = \frac{-T_s}{\ln(-a_1)} \quad (13)$$

The discrete form of the controller is synthesized with the next expression:

$$C(z) = K_c \frac{r_0 z + r_1}{z + r_2} \tag{14}$$

where $r_0 = a$, $r_1 = -a + (1 - e^{-T_s/T})$ and $r_2 = -e^{-T_s/T}$. The control signal can be indicated by the recurrent equation:

$$u(k) = r_2 u(k-1) + r_0 e(k) + r_1 e(k-1) \tag{15}$$

To validate the proposed controller, closed-loop output responses are highlighted in **Figure 7**, which demonstrates ability of the adaptive phase lead control to maintain closed-loop performances considering the system parameters' variation.

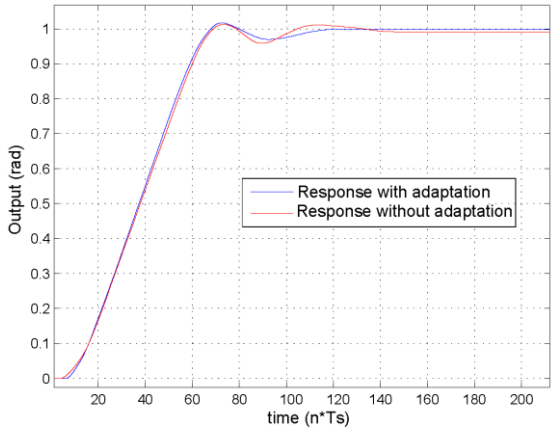

Figure 7 Closed-loop responses with and without adaptation.

Analog-analog adaptive lead control

Controllers in digital form offer various benefits compared to completely analog controllers. The main merit of numerical commands is the versatility of adjustment of control parameters. The electric consumption, the weight and the congestion are all reduced with a noticeable insensitivity against temperature change. Likewise, digital controllers exhibit a dynamic deterioration in view of the delays of analog-digital conversion and control algorithm execution, and they can be more important with the decrease of sample frequency, **Figure 8**.

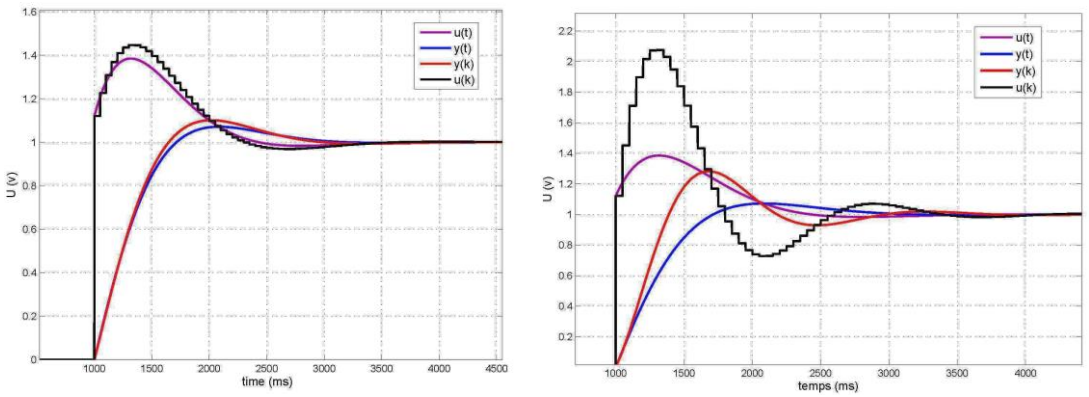

Figure 8 Analog-digital comparison.

A small non-linearity can appear owing to analog-digital conversion where the output *y(t)*, that will not be the exact value at the time *kTe*, can generate few oscillations increasing mostly with low resolution conversion. In digital control, the measure acquisition and the control update are performed each period. From this perspective, between *kTe* and *(k + 1)Te*, the system remains in open loop. Even though this interval maintains frequently small values compared to process dynamic, disturbances can only be detected at the interval end triggering a serious risk in some cases.

The analog architecture of the adaptive phase lead controller is illustrated in **Figure 9**. In this structure, digital potentiometers are used to adjust transfer function parameters with a right approximation:

$$a(k) = \frac{R_1(k)C_1}{R_2(k)C_2}$$
$$K_c(k) = \frac{R_3(k)}{R_4(k)}$$
$$T(k) = R_2(k)C_2 \quad (16)$$

Another analog architecture based on operational amplifiers is also established to design the system as reported in **Figure 9**.

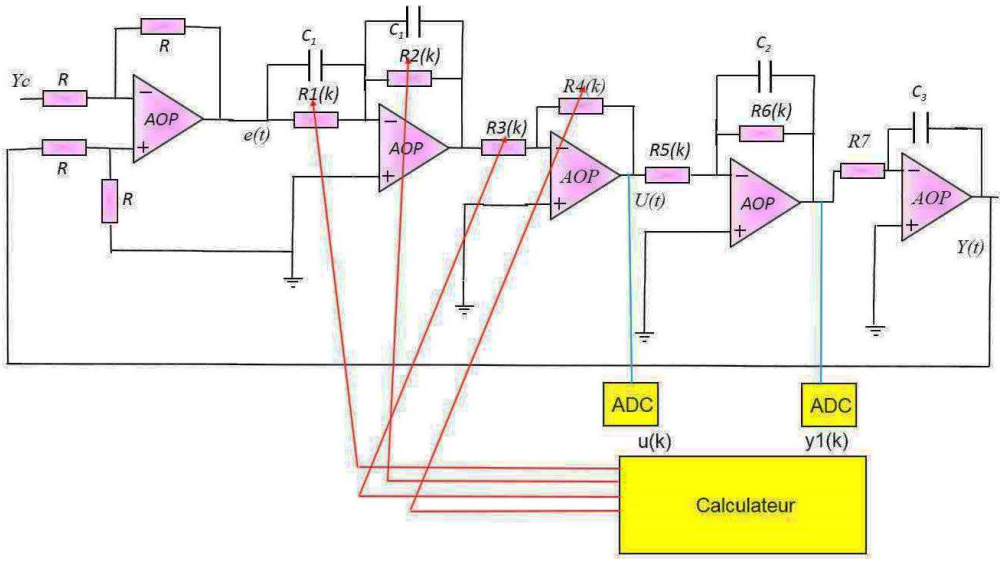

Figure 9 Adaptive analog control loop.

The transfer function deduced from the electronic circuit is equivalent to a 1st order system multiplied by an integral similar to the robot transfer function (Eq. (5)), where $\tau = R_6(k)C_2$ and $K = \frac{R_6(k)}{R_5(k)}$. Therefore, the analog adaptive control loop is composed of the controller and the process designed with operational amplifiers and programmable resistors, **Figure 9**. Continuous parameters are generated from discrete parameter estimation. The gain and the constant time display the following expressions:

$$K(k) = \frac{b_1(k)}{1 + a_1(k)} \text{ and } \tau(\mathrm{k}) = \frac{-T_s}{\ln(-a_1(k))} \quad (17)$$

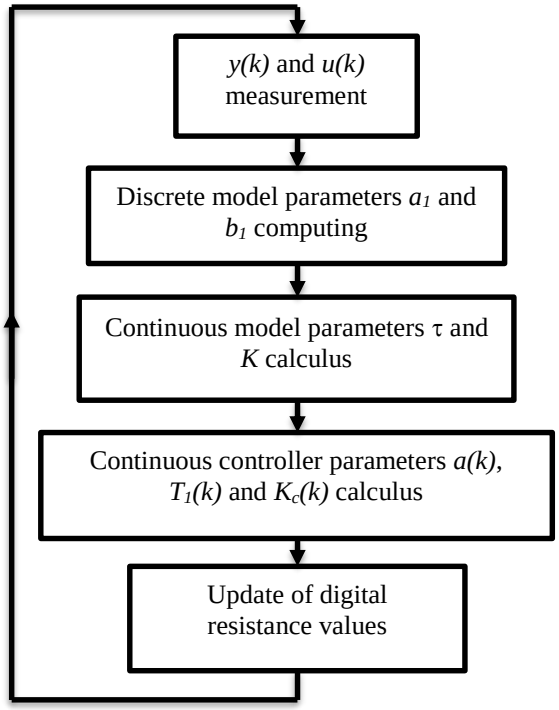

Figure 10 Control algorithm.

To return to the continuous form, an update of the controller parameters is required to elaborate the controller form in terms of:

$$C(p) = K_c(k)\frac{1+a(k)T(k)p}{1+T(k)p} \tag{18}$$

The compensation of $\tau(k)$ by $a(k)T(k)$ yields the following expressions:

$$K_c(k) = \frac{\omega_n}{2\xi K(k)} \tag{19}$$

$$T(k) = \frac{K(k)K_c(k)}{\omega_n^2} \tag{20}$$

On the other side, the equality $a(k)T(k) = R_1(k)C_1$ allows to obtain:

$$R_1(k) = \frac{a(k)T(k)}{C_1} \tag{21}$$

$$R_2(k) = \frac{T(k)}{C_2} \tag{22}$$

To validate the proposed approach in real time tests, a control algorithm is developed depending on the sampling period. It is depicted in **Figure 10**.

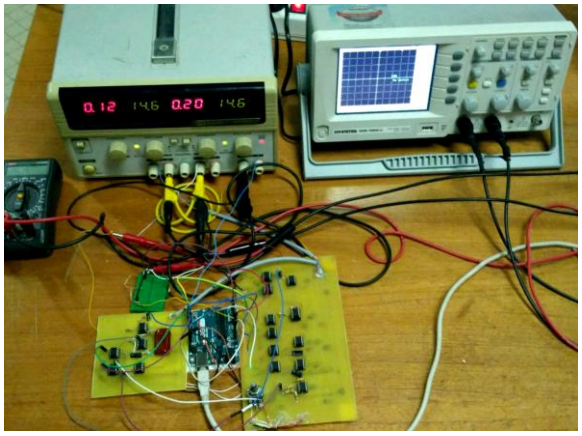

Figure 11 Adaptive test bed control.

The entire real prototype carried out in our Laboratory is portrayed in **Figure 11**, where the start-up controller is synthesized for a nominal gain K_n and a nominal time constant τ_n to obtain a closed-loop order system with $\xi = 1$ and $\omega_n = rad/s$. The consign "1V step signal" is chosen. In **Figure 12**, for a stationary system, the output response indicated by a blue line guarantees a good performance and the control signal in yellow expresses an acceptable variation.

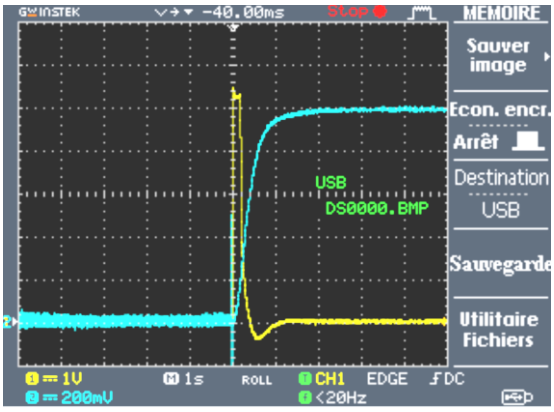

Figure 12 Stationary system output.

Different experiments are conducted with uncertainties onto gain, time constant and both for different ways of variation. In the 1st case, the analog simulator presents uncertainty on gain as:

$$G_1(p) = \frac{5K_n}{p(1+\tau_n p)} \tag{23}$$

Figure 13 presents an output with an adequate pursuit and an overshooting attenuation. To perform a pertinent evaluation of the adaptive controller, an uncertainty on time constant of the analog simulator is determined as follows:

$$G_2(p) = \frac{K_n}{p(1+\frac{\tau_n}{2} p)} \tag{24}$$

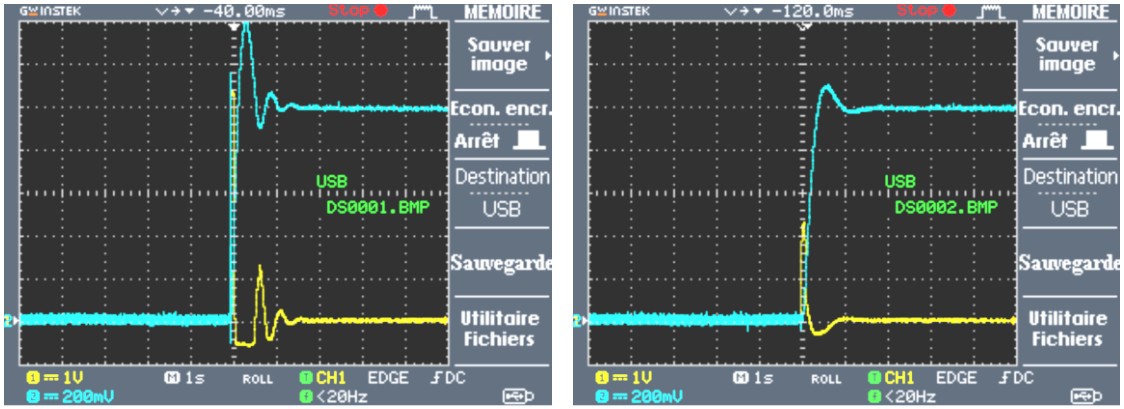

Figure 13 System outputs with uncertainty on gain.

The output evolution of the adaptive controlled system provided in **Figure 14** presents a rapidity improvement with a closed-loop performances holding.

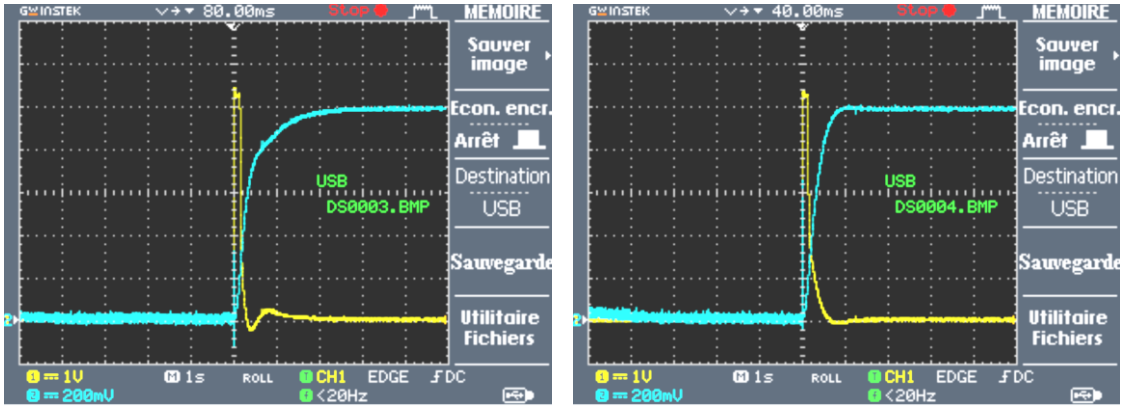

Figure 14 System outputs with uncertainty on time constant.

Two cases of adaptive controller offering uncertainties in gain and time constant with different directions of variation are reported in **Figure 15**, with transfer functions specified as:

$$G_3(p) = \frac{K_n/2}{p(1+\frac{\tau_n}{2}p)} \tag{25}$$

$$G_4(p) = \frac{5K_n}{p(1+\frac{\tau_n}{2}p)} \tag{26}$$

Despite various uncertainties applied to model parameters, the adaptive controller ensures closed-loop performances and improves efficiency in both accuracy and dynamics.

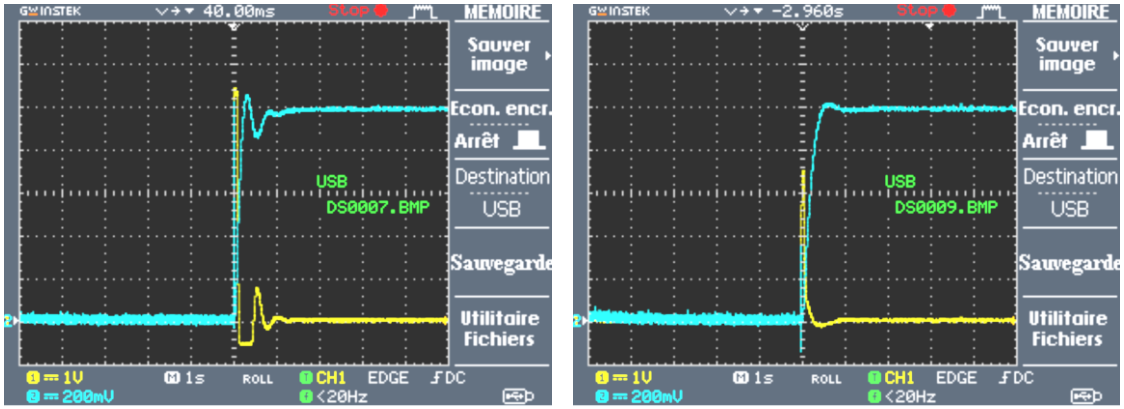

Figure 15 System outputs with uncertainty on gain and time constant.

Conclusions

This work tackles 2 approaches of adaptive phase lead control applied to ALV systems presenting uncertainties owing to soil nature change. The 1st control law, completely digital, can ensure closed-loop performances in the case of model parameters variation. The 2nd approach is an analog adaptive control based on programmable resistances. Both methods are elaborated and assessed in real time to corroborate efficiency in different cases of model uncertainties in order to resolve uncertain parameters of ALV models.

Acknowledgements

This work was supported by the Ministry of the Higher Education and Scientific Research in Tunisia.

References

[1] Z Huang, X Xu, H He, J Tan and Z Sun. Parameterized batch reinforcement learning for longitudinal control of autonomous land vehicles. *IEEE Trans. Syst. Man Cybern. Syst.* 2017; **49**, 730-41.

[2] AD Luca, G Oriolo and M Vendittelli. *Control of wheeled mobile robots: An experimental overview*. *In*: S Nicosia, B Siciliano, A Bicchi and P Valigi (Eds.). Ramsete. Springer, Berlin, Heidelberg, Germany, 2001, p. 181-226.

[3] P Coelho and U Nunes. Path-following control of mobile robots in presence of uncertainties. *IEEE Trans. Robot.* 2005; **21**, 252-61.

[4] P Lamon and R Siegwart. Wheel torque control in rough terrain-modelling and simulation. *In*: Proceedings of the IEEE International Conference on Robotics and Automation, Barcelona, Spain. 2005, p. 867-72.

[5] L Caracciolo, AD Luca and S Iannitti. Trajectory tracking control of a four-wheel differentially driven mobile robot. *In*: Proceedings of the IEEE International Conference on Robotics and Automation, Detroit, Michigan. 1999, p. 2632-8.

[6] ML Corradini and G Orlando. Control of mobile robots with uncertainties in the dynamical model: A discrete time sliding mode approach with experimental results. *Control Eng. Pract.* 2002; **10**, 23-34.

[7] W Dong and KD Kuhnert. Robust adaptive control of nonholonomic mobile robot with parameter and nonparameter uncertainties. *IEEE Trans. Robot.* 2005; **21**, 261-6.

[8] ZP Jiang and H Nijmeijer. Tracking control of mobile robots: A case study in backstepping. *Automatica* 1997; **33**, 1393-9.

[9] BS Park, SJ Yoo, JB Park and YH Choi. Adaptive neural sliding mode control of nonholonomic wheeled mobile robots with model uncertainty. *IEEE Trans. Control Syst. Technol.* 2009; **17**, 207-14.

[10] MS Kim, JH Shin, SG Hong and JJ Lee. Designing a robust adaptive dynamic controller for nonholonomic mobile robots under modelling uncertainty and disturbances. *Mechatronics* 2003; **13**, 507-19.

[11] AK Khalaji. Modelling and control of uncertain multibody wheeled robots. *Multibody Syst. Dyn.* 2019; **46**, 257-79.
[12] N Lobontiu. *Time- and frequency-domain controls of feedback systems*. *In*: System dynamics for engineering students, Academic Press, London, 2018, p. 647-708.
[13] W Bolton. *Frequency response*. *In*: Instrumentation and control systems. 3rd eds. Newnes, Oxford, 2021, p. 257-86.